Genome-wide CRISPR-Cas9 screen reveals common factors in dsRNA and Sindbis virus-induced cell death

Olivier Petitjean[1, *], Erika Girardi[1, *], Richard Patryk Ngondo[2], Vladimir Lupashin[3], Sébastien Pfeffer[1, ‡]

1 Université de Strasbourg, Architecture et Réactivité de l'ARN, Institut de biologie moléculaire et cellulaire du CNRS, 2 allée Konrad Roentgen, 67084 Strasbourg France

2 Université de Strasbourg, Institut de Biologie Moléculaire des Plantes du CNRS, 12 rue du Général Zimmer, 67084 Strasbourg France

3 University of Arkansas for Medical Sciences, 4301 West Markham Street, Little Rock, Arkansas 72205, United States of America

* These authors contributed equally

‡ To whom correspondence should be addressed: spfeffer@unistra.fr

Abstract

Double stranded RNA (dsRNA) is the hallmark of many viral infections. dsRNA is produced either by RNA viruses during replication or by DNA viruses upon convergent transcription. Synthetic dsRNA is also able to mimic viral-induced activation of innate immune response and cell death. In this study, we employed a genome-wide CRISPR-Cas9 loss of function screen based on cell survival in order to identify genes implicated in the host response to dsRNA. By challenging HCT116 human cells with either synthetic dsRNA or Sindbis virus (SINV), we identified the heparan sulfate (HS) pathway as a crucial factor for dsRNA entry and we validated SINV dependency on HS. Interestingly, we uncovered a novel role for COG4, a component of the Conserved Oligomeric Golgi (COG) complex, as a factor involved in cell survival to both dsRNA and SINV. We showed that COG4 knock-out led to the depletion of extracellular HS, specifically affected dsRNA transfection efficiency and reduced viral production, explaining the increased cell survival of these mutants.

Importance

When facing a viral infection, the organism has to put in place a number of defense mechanisms in order to get rid of the pathogen. At the early phase of this preparation for fighting against the invader, the innate immune response is triggered by the sensing of danger signals. Among those molecular cues, double-stranded (dsRNA) is a very potent inducer of different reactions at the cellular level that can ultimately lead to cell death. Using a genome-wide screening approach, we set to identify the genes involved in dsRNA sensing and apoptosis induction in human cells. This allowed us to determine that the heparan sulfate pathway, and the Conserved Oligomeric Golgi complex, are key determinants allowing both cellular entry of dsRNA and subsequent signaling leading to cell death.

Introduction

When a virus infects a cell, numerous mechanisms are put in place to raise the alarm and get rid of, or at least limits, the invader. One of the first barrier that the virus has to overcome to is to enter the cell by taking advantage of wide diversity of ubiquitous or cell-specific cellular receptors. In addition to protein receptors, glycosaminoglycans present at the cell surface also represent crucial factors for efficient viral attachment and entry (Bomsel and Alfsen, 2003). Glycosaminoglycans, and more precisely heparan sulfates are ubiquitously expressed in human cells. They possess a global negative charge that is able to interact electrostatically with the basic residues that are exposed by viral surface glycoproteins. This allows viruses to increase their concentration at cell surface and so the possibility to interact with their specific entry receptor (Rusnati et al., 2009). For instance, alphaviruses such as Semliki Forest virus (SFV) and Sindbis virus (SINV) are enveloped positive-strand RNA viruses that contain two glycoproteins at the envelope, the proteins E1 and E2. E2 is involved in the interaction of the virus particle to the cell surface (Byrnes and Griffin, 1998; Smith et al., 1995), while E1 serves in the fusion process (Wahlberg et al., 1992).

Once inside the cell, the replication of the viral genome represents another critical step to trigger the antiviral immune response. A ubiquitous pathogen-associated molecular pattern (PAMP) recognized by the cellular machinery is double-stranded (ds) RNA, which can arise as a replication intermediate for viruses with an RNA genome, or from convergent transcription for DNA viruses (Weber et al., 2006). In mammals, dsRNA recognition is driven by specific receptors including the cytoplasmic RIG-Like Receptors (RLRs) and endosomal Toll Like Receptors (TLRs) (Schlee and Hartmann, 2016). Sensing of dsRNA by these receptors results in the activation of a complex signaling cascade leading to the production of type I interferon (IFN), which in turn triggers the expression of IFN stimulated genes (ISG) and the establishment of the antiviral state (Stetson and Medzhitov, 2006). The ultimate outcome of

this vertebrate-specific antiviral response is translation arrest and cell death by apoptosis (García et al., 2007).

The revolution brought by the discovery of the CRISPR-Cas9 technology has provided biologists with an invaluable tool to edit the genome at will and easily perform individual gene knock-out (Shalem et al., 2015). This technique is perfectly suited to perform genome-wide screens in a relatively fast and easy to implement manner, especially when the readout is based on cell survival. For this reason, numerous CRISPR-Cas9 loss of function screens have been performed based on cell survival after infection with different viruses (Han et al., 2018; Park et al., 2017; Zhang et al., 2016). These approaches allowed the identification of novel virus specific as well as common factors involved in antiviral defense mechanisms or in cellular permissivity to virus infection.

Here, we chose to take advantage of the fact that dsRNA is almost always detected in virus-infected cells (Weber et al., 2006) and is a potent inducer of apoptosis to design a genome-wide screen aiming at identifying host genes that when edited resulted in increased cell survival to dsRNA and viral challenge. To this aim, we performed a CRISPR-Cas9 screen based on cell survival in HCT116 cells after either cationic lipid-based transfection of an *in vitro* transcribed long dsRNA or infection with the model alphavirus SINV, which replicates *via* a dsRNA intermediate.

Our results indicate that genes involved in limiting attachment and therefore entry, be it of the synthetic dsRNA or SINV, are vastly over-represented after selection. We validated two genes of the heparan sulfate pathway (namely *SLC35B2* and *B4GALT7*) as required for dsRNA transfectability and SINV infectivity. We also identified and characterized COG4, a component of the conserved oligomeric golgi (COG) complex, as a novel factor involved in resistance to dsRNA and viral infection via the heparan sulfate biogenesis pathway, although not

exclusively. Altogether, these findings demonstrate that the identification of key pathways of the cellular response to RNA virus can be achieved by employing synthetic dsRNA as a tool.

Results

Genome-wide CRISPR/Cas9 screen based on cell survival upon dsRNA transfection identify factors of the heparan sulfate pathway

In order to identify cellular genes that are involved in the cellular response to dsRNA which culminates with cell death, we performed a CRISPR/Cas9 genome-wide loss-of-function screen in the human colon carcinoma cell line HCT116. This cell line is highly suitable for CRISPR/Cas9 genetic screening procedures (Golden et al., 2017) and can be easily infected with SINV (Fig. S1A). We also showed that complete cell death could be achieved within 48 hours in unedited HCT116 cells upon transfection of an *in vitro* transcribed long dsRNA of 231 bp by a cationic lipid-based transfection reagent (Fig. S1B).

We generated a Cas9-expressing HCT116 polyclonal cell line that we stably transduced with the human genome-wide lentiviral Brunello library composed of 76 441 gRNAs targeting 19 114 genes (Doench et al., 2016). We then applied a positive selection by lipofecting the transduced cells with the synthetic long dsRNA and surviving cells were collected 48h later.

Libraries from input genomic DNA and from the surviving cells were generated and sequenced (Fig. 1A). We identified eight genes that were statistically enriched using the MAGeCK software (Li et al., 2014). Among those, four genes belonged to the heparan sulphate biosynthesis pathway (namely, *SLC35B2*, *B4GALT7*, *EXT1* and *EXT2*) and three were components of the oligomeric golgi complex (namely *COG3*, *COG4* and *COG8*) (Fig. 1B & Dataset S1).

Heparan sulphate (HS) is a linear polysaccharide that is covalently attached to core proteins in proteoglycans (PG) on the cell surface (for review, see Li and Kusche-Gullberg, 2016). Among

many properties, HS play a role in binding of protein ligands and as a carrier for lipases, chemokines and growth factor (Bishop et al., 2007; Li and Kusche-Gullberg, 2016), but also as a viral receptor (Cagno et al., 2019). HS biosynthesis takes place in the Golgi, where most of the biosynthetic enzymes are anchored to the Golgi membrane (Lindahl et al., 2015).

We first validated the resistance phenotype to dsRNA of *SLC35B2* and *B4GALT7*, the two top hits identified in the screen, by generating two individual knock-out clones for each gene by CRISPR-Cas9 editing in HCT116cas9 (Fig. S2). Knock-out of both *SLC35B2* and *B4GALT7* genes abolished cell death induced by dsRNA lipofection compared to wild-type HCT116 cells, as assessed by the measurement of cell viability 48h post transfection (Fig. 1C, left panel). These results confirm our genome-wide approach based on cell survival and directly demonstrate the involvement of *SLC35B2* and *B4GALT7* in dsRNA-induced cell death. The observed resistance to dsRNA in the mutants could occur at many different steps: dsRNA liposome attachment and entry, recognition, induction of the IFN pathway or apoptosis. To test whether the first step was affected, we employed a nucleic acid delivery method that was not based on cationic lipid transfection. In particular, we used nucleofection (an electroporation-based transfection method) to introduce dsRNA into HCT116 cells and we showed that this approach totally restored cell death in *SLC35B2* and *B4GALT7* knock-out cells (Fig. 1C, right panel). We also confirmed that liposome-based transfection of nucleic acid was impaired in *SLC35B2* and *B4GALT7* KO cells, by transfecting a GFP-expressing plasmid using either Lipofectamine 2000 or nucleofection in wild type or knock-out cells. As shown in Fig. 1D, GFP could be detected in all conditions upon electroporation, but not when the plasmid was lipofected. In addition, liposome-based transfection of *in vitro* transcribed Cy5-labelled dsRNA was also abolished in *SLC35B2* and *B4GALT7* KO cells as assessed by FACS measurement of fluorescence 48 h post-transfection (Fig. S3A).

To establish whether impairment of the HS synthesis is directly linked to a defect in dsRNA entry and increased cell survival, we measured the extracellular HS levels in *SLC35B2* and *B4GALT7* KO cells. We measured a substantial reduction of the extracellular HS staining as assessed by FACS measurement of two independent *SLC35B2* and *B4GALT7* KO clones compared to HCT116 wild type cells (Fig. 1E). To confirm the importance of HS at the cell surface for liposome-based transfection, we mimicked the HS-defective phenotype by removing extracellular HS in parental HCT116cas9 cells either enzymatically (with heparinase) or chemically (with sodium chlorate NaClO3). We then tested the cell transfectability of a GFP-expressing plasmid. In agreement with our hypothesis, the heparinase treatment recapitulates the defect in lipofection observed in *SLC35B2* and *B4GALT7* KO cells (Fig. 1F) by removing extracellular HS (Fig. S3B) and formally demonstrates that extracellular HS are crucial for transfection by lipofection. Similarly, the treatment of cells with NaClO3 abolished the GFP plasmid transfection (Fig. 1G). However, in the latter case, this did not correlate with a decrease in overall extracellular HS (Fig. S3C). This could be due to the fact that while a mix of heparinase I & III remove every kind of extracellular heparan sulfates, 50 mM of NaClO3 only impairs the O-sulfation (Safaiyan et al., 1999). Taken together, our results show that knocking out *SLC35B2* and *B4GALT7* results in reduced levels of extracellular HS, which in turn impairs liposome-based transfectability of HCT116 cells. Moreover, the validation of these two top hits indicates that other candidates might be suitable for further analysis and may also have an impact on the dsRNA resistance phenotype

COG4 is involved in dsRNA-induced cell death partly via the heparan sulphate pathway

Among the first hits of our genome-wide screen were proteins related to COG complex, namely COG4, COG3 and COG8. The COG complex is a hetero-octameric complex containing 8 subunits (COG1-8) interacting with numerous proteins mainly involved in intra-Golgi

membrane trafficking such as vesicular coats, Rab proteins and proteins involved in SNARE complex (Blackburn et al., 2019; Willett et al., 2013). This interaction with the trafficking machinery is crucial for the proper functionality of the Golgi apparatus and mutations in the COG complex result in severe cellular problems such as glycosylation defect (Kranz et al., 2007; Reynders et al., 2009a; Spaapen et al., 2005; Zeevaert et al., 2008), which are due to mislocalization of recycling Golgi enzymes (Shestakova et al., 2006; Zolov and Lupashin, 2005).

Since we retrieved three out of the eight COG family members in our CRISPR/Cas9 screen suggesting their importance in dsRNA-induced cell death, we tested the effect of their inactivation by CRISPR-Cas9 in previously generated HEK293T cells (Bailey Blackburn et al., 2016). In particular, loss of function *COG4* mutants displayed the most significant survival phenotype in response to dsRNA lipofection and this phenotype could be complemented by stable expression of a COG4-GFP construct (Fig 2A). In order to assess whether the *COG4* KO survival phenotype was associated with the heparan sulphate pathway defect, we stained extracellular HS and measured the HS profile by FACS analysis. We observed a decrease of extracellular HS in KO *COG4* cells compared to control cells (WT and rescued) which confirms that the COG complex is related to the HS biosynthesis pathway (Fig 2B).

We then asked if this HS reduction correlated with a decrease in transfectability due to an extracellular HS depletion in KO *COG4* cells. Surprisingly, lipofection of a GFP expressing plasmid in these cells indicated that HEK293T *COG4* KO cells are still transfectable with plasmid DNA as observed by epifluorescence microscopy (Fig 2C) and FACS analysis (Fig. S4A). On the contrary, dsRNA transfectability appeared to be significantly reduced in HEK293T KO *COG4* cells compared to control cells as determined by RT-qPCR analysis of dsRNA isolated from cells 24h after transfection (Fig 2D). In parallel, we also performed transfection of Cy5-labelled dsRNA and observed a strong reduction of Cy5 signal in KO cells

compared to WT or rescued cells as measured by FACS analysis (Fig. S4B). In order to better assess to which extent dsRNA internalization was altered in *COG4* KO cells, we performed dsRNA immunofluorescence analysis in HEK293T *COG4* KO or rescued cells 24 h after dsRNA transfection. The results indicate that dsRNA could be still detected in *COG4* KO cells suggesting that dsRNA transfectability is strongly reduced but not totally impaired in the absence of COG4 (Fig. 2E). We confirmed these findings by transfecting rhodamine-labeled poly(I:C), a synthetic analog of dsRNA in HEK293T *COG4* KO or WT cells (Fig. S4C) and by counting the number of poly I:C foci per cell at 6, 12 and 24 h post transfection (Fig. S4D).

Upon dsRNA sensing, the interferon-induced proteine kinase R (PKR) phosphorylates the translation initiation factor EIF2α in order to block cap-dependent translation and induce apoptosis in wild-type cells. In order to verify whether the few dsRNA molecules inside the cells were still able to activate a functional IFN pathway, we measured EIF2α phosphorylation state upon dsRNA treatment and observed that this modification was still present in HEK293T *COG4* KO cells despite the reduced cell death phenotype (Fig. 3F). Altogether these findings indicate that the COG complex is involved in HS biosynthesis and that removal of *COG4* results in a lower accumulation of HS at the cell surface, which most likely translate in a reduced transfectability of dsRNA. However, as opposed to the observations in *SLC35B2* or *B4GALT7* KO cells, the cell survival phenotype in COG4 KO cells is associated to a reduced but not completely abolished dsRNA internalization. This seems specific to RNA molecules as DNA transfection efficiency seems to be preserved. Finally, the failure of apoptosis induction upon dsRNA transfection does not correlate with an impaired type I IFN activation since EIF2α phosphorylation is maintained in *COG4* KO cells.

Cell survival based genome-wide CRISPR/Cas9 screen identifies *COG4* as a permissivity factor to SINV

SINV is a small enveloped virus with a single stranded RNA genome of positive polarity. The virus belongs to the *Togaviridae* family, alphavirus genus and is considered as the model for other medically important viruses such as chikungunya virus (CHIKV) and Semliki forest virus (SFV). During its infectious cycle, SINV produces dsRNA as a replication intermediate and induces cytopathic effects in mammalian cells, leading to cell death within 24 to 48 h post-infection (Strauss and Strauss, 1994).

In order to identify host genes that are critical for SINV infection, we performed a CRISPR/Cas9 knock-out screen in HCT116 cells, which are susceptible to this virus (Fig 3A & Dataset S2). After transduction with the CRISPR lentiviral genome-wide knockout library, puromycin-resistant HCT116 cells were infected with SINV-GFP at a MOI of 0.1. *SLC35B2* and *B4GALT7* were identified as top hits of this second screen (Fig 3B). Genes of the heparan sulphate pathway have been previously found in genome-wide CRISPR-Cas9 loss of function studies looking for factors involved in the accumulation of viruses such as Influenza, Zika and chikungunya (Han et al., 2018; Li et al., 2019; Tanaka et al., 2017). Interestingly, among the top-ranking hits, we retrieved *COG4* which was not previously associated with SINV infection. To validate the involvement of *COG4* upon SINV infection, we infected WT and *COG4* KO HEK293T cells with SINV-GFP. We observed that GFP accumulated to lower levels in *COG4* KO than in WT cells both at 24 and 48 h post-infection (hpi) (Fig. 3C). In addition, the determination of viral titer by plaque assay showed that *COG4* KO cells produced less infectious viral particles than WT or *COG4*-rescued cells both at 24 and 48 hpi (Fig. 3D). In order to test whether the reduced viral production in KO *COG4* cells was associated with a reduced accumulation of viral dsRNA in the cytoplasm, we infected WT or *COG4* KO cells with SINV-GFP and performed immunostaining with the anti-dsRNA J2 antibody 24 hpi. We observed a reduction of the J2 staining in terms of number of positive cells in the *COG4* KO

condition (Fig. 3E). Overall, our results indicate that COG4 expression is needed for an efficient SINV infection, which might be linked with its involvement in the HS biosynthesis pathway.

Discussion

Several CRISPR/Cas9 screens aiming at identifying factors required for infection by specific viruses have been described in the literature, but to our knowledge, none has been designed to look at the effect of the only common factor between all those viruses, *i.e.* dsRNA. Here, we used the Brunello gRNA lentiviral library to screen for genes involved in HCT116 cells survival to synthetic dsRNA transfection and to SINV infection. This allowed us to identify components of the heparan sulphate biosynthesis pathway and of the COG complex as critical host factors in the cellular response to above mentioned challenges. It has been already reported that cell-survival-based CRISPR screens for viral host factors are biased toward genes linked to the initial steps of the infection, and even more so to viral entry (Han et al., 2018; Savidis et al., 2016). Thus, in our case, HS is a well-known factor required for SINV entry due to the virus adaptation to cell culture (Klimstra et al., 1998). We also retrieved genes of the HS pathway in our dsRNA-based screen, and we confirmed the importance of extracellular HS for dsRNA-induced toxicity. This is mostly due to a decrease of transfectability of the cells when HS are missing, which is linked to the fact that the polyplexes used for transfection are positively charged and can interact electrostatically with glycosaminoglycans (Mislick and Baldeschwieler, 1996; Payne et al., 2007). This part of our work also points out to the limitations of survival-based CRISPR-Cas9 screens, *i.e.* the selection pressure is too strong to allow the identification of genes intervening after the entry step, thereby making the screen less sensitive. New strategies should be designed to overcome this problem, such as using fluorescent-based cell sorting in order to be less stringent in the selection.

In addition to the HS pathway, we identified members of the COG complex, and more specifically *COG4*, as factors involved in dsRNA transfection and SINV infection. Loss of

function COG4 mutant cells show a dsRNA-resistant phenotype as well as a reduction in extracellular HS expression, similar to previously published reports for other COG proteins (Jae et al., 2013; Tanaka et al., 2017). Surprisingly, even if the removal of COG4 expression results in a defect in the HS pathway, we are still able to transfect the KO COG4 cell line either with a plasmid encoding GFP or, although to a lesser extent, dsRNA. In addition, the dsRNA molecules that are able to enter into HEK293T KO *COG4* are still sufficient to lead to the phosphorylation of EIF2A, indicating that the innate immune response is not totally abrogated. Nonetheless, cell death induced by dsRNA appears to be lower in *COG4* KO cells. Our CRISPR/Cas9 screen using SINV as a challenge also identified *COG4* as a new factor involved in cell survival to SINV infection. The infection kinetic of SINV seems to be delayed, but not totally impaired, in *COG4* KO cells. However, cells again appear to survive longer to the virus infection. Future work will be needed in order to assess whether this phenotype upon SINV infection is only correlated with a defect in HS biogenesis in *COG4* mutants. The fact that *COG4* KO cells seem to better survive to both synthetic dsRNA transfection and viral infection opens several interesting perspectives. Indeed, since the COG complex is related to glycosylation and membrane trafficking (Blackburn et al., 2018a; Reynders et al., 2009b; Ungar et al., 2002; Willett et al., 2013), deficiency in one or more of its components could lead to a glycosylation and/or subcellular localization defect of components of the innate immune response or of the apoptosis pathway. The difference of transfectability of plasmid DNA and dsRNA in *COG4* KO cells is also intriguing and could indicate that different kinds of nucleic acids to not necessarily use the exact same routes to enter the cells upon liposome-based transfection. Finally, there could be other defects linked to COG deficiencies (D'Souza et al., 2019; Blackburn et al., 2018b) that could account for our observations and elucidating those will require further work.

In conclusion, our work uncovered *COG4* as a new player in the HS production, which is required for both SINV infection and dsRNA transfection, and expanded the function of the COG to nucleic acids based innate immunity. These results also highlight that synthetic dsRNA is a powerful tool to identify novel key pathways of the cellular response to RNA virus.

Materials and Methods

Cell culture and virus

HCT116, HEK293T, HEK293T COG KOs, BHK21 and Vero R cells were maintained in Dulbecco's Modified Eagle Medium (DMEM) 4.5 g/L glucose (Gibco, Thermo Fisher Scientific Inc.) supplemented with 10% fetal bovine serum (FBS) (Takara) in a humidified atmosphere of 5% CO_2 at 37°C. HEK293T *COG3*, *COG8* and *COG4* KO and *COG4* KO stably rescued with COG4-GFP were described previously (Climer et al., 2018; Blackburn and Lupashin, 2016). HCT116cas9 and HEK293T COG4rescued were maintained in the same medium with addition of 10 ug/mL blasticidine. HCT116 KO clones (*SLC35B2*#1 and #2, *B4GALT7*#1 and #2 were maintained in the same medium with addition of 10 ug/mL blasticdine and 1 ug/mL puromycine.

SINV wilde type (SINV) or expressing the green fluorescent protein (SINV-GFP) were produced as previously decribed (López et al., 2020) in BHK21 cells. Cells were infected with either SINV WT or SINV GFP at a MOI of 10^{-1} and samples were harvested at 24 or 48 hours post-infection (hpi).

Standard plaque assay

10-fold dilutions of the viral supernatant were prepared. 50 μl aliquots were inoculated onto Vero R cell monolayers in 96-well plates for 1 hour. Afterwards, the inoculum was removed and cells were cultured in 2.5% carboxymethyl cellulose for 72 h at 37ºC in a humidified

atmosphere of 5% CO_2. Plaques were counted manually under the microscope. For plaque visualization, the medium was removed, cells were fixed with 4% formaldehyde for 20 min and stained with 1x crystal violet solution (2% crystal violet (Sigma-Aldrich), 20% ethanol, 4% formaldehyde).

J2 immunostaining

Wild-type or KO *COG4* HEK293T cells were plated on millicell EZ slide (Millipore) and were transfected with 1 μg/mL of IVT dsRNA or infected with SINV at an MOI of 0.1 for 24h. Non transfected and mock-infected cells were used as control, respectively. Cells were fixed with 4% formaldehyde diluted in PBS 1x for 10 min at room temperature, followed by incubation in blocking buffer (0.2% Tween X-100; PBS 1x; 5% normal goat serum) for 1 h. J2 antibody (Scicons) diluted in blocking buffer at 1:1000 was incubated over night at 4°C. Between each steps, cells were washed with PBS 1X-Tween 0.2%. Secondary antibody goat anti-mouse Alexa 594 (ThermoFisher) diluted at 1:1000 in PBS 1x-Tween 0.2% were incubated for 1 h at room temperature. After DAPI staining (1:5000 dilution in PBS 1x for 5 min), slides were mounted with a coverslip over anti-fading medium and observed by epifluorescence microscopy using the BX51 (Olympus) microscope with a X 40 objective.

Generation of HCT116cas9 line.

The HCT116cas9 cells, expressing human codon-optimized S. pyogenes Cas9 protein, were obtained by transducing wild type HCT116 colorectal carcinoma cell line (ATCC® CCL-247™) with lentiCas9-Blast lentiviral vector (Addgene #52962). Briefly, wild-type HCT116 cells were cultured in standard DMEM (GIBCO) medium supplemented with 10% Fetal bovine serum (FBS, Gibco) and 100 U/mL of penicillin-Streptomycin (Gibco) at 37°C in 5% CO_2. The cells were transduced at 80% confluency in a 10 cm tissue culture plate, using 6 mL lentiviral

supernatant supplemented with 4μg/mL of polybrene (H9268, sigma) for 6 hours. The transduction medium was replaced with fresh growing medium for 24h before starting the selection. Transduced HCT116cas9 cells were selected for 10 days and maintained in growing medium supplemented with 10μL/mL of Blasticidin (Invivogen).

High titer lentiviral sgRNA library production.

The production of high titer Human sgRNA Brunello lentiviral library which contains 4 sgRNA per gene (Doench et al 2018) (Addgene #73178), was performed by transfecting HEK293T cells in five 15 cm tissue culture plates using PEI (Polyethylenimin Linear, MW 25,000, 23966-1-A, Polysciences) transfection method (Boussif et al 1995). Briefly, for each 15 cm plate containing 20 mL of medium, 10μg of sgRNA library, 8μg of psPAX2 and 2μg of pVSV diluted in 500μL of NaCl 150 mM were combined with 40μL of PEI (1.25 mg/mL) dissolved in 500μL of NaCl 150 mM. The mix was incubated 30 minutes at room temperature and the formed complexes were added dropwise on the cells. After 6 hours, the medium was replaced and the viral supernatant was collected after 48 hours and after 72 hours. The supernatant was filtered through a 0.45μm PES filter and the viral particles concentrated 100 times using Lenti-X™ Concentrator (Takara) before storage at -80. The viral titer was established by counting puromycin resistant colonies formed after transducing HCT116 cells with serial dilutions of viral stock. HCT116cas9 cells were transduced with lentivirus-packaged Brunello sgRNA library at a MOI of 0.3. The lentiviral library has been sequenced to verify that all the lenti-gRNA are represented.

Genome-wide CRISPR/Cas9 knock-out screens.

For each replicate (n=3), 5x10^6 cells/dish were seeded in 6x15cm^2 plate in order to keep a 300X representattivity of the sgRNA library. Input samples were collected as controls. One day later,

cells were either lipofected with 1 ug/mL dsRNA-Citrine or infected with SINV at MOI of 0.1 and cultured at 37°C 5% CO_2. Cells were washed with PBS 1X 48 hours post treatment, to remove dead cells and fresh media was added to surviving clones. Cells were expanded and collected 6 days post dsRNA transfection and 18 days post SINV infection.

Genomic DNA was isolated by resuspending the cell pellet in 5 mL of resuspension buffer (50 mM Tris-HCl pH 8.0, 10 mM EDTA, 100 µg/ml RNaseA), 0,25 mL of 10% SDS was added and incubated 10 mins at RT after mix. After incubation, the sample was sonicated and incubated 30 mins at RT with 10 uL of proteinase K (10mg/mL). 5 mL of Phenol/Chloroform/Isoamyl Alcohol solution was added and followed by a spin down 60 mins at 12000g/20°C. Upper phase was transferred into a new tube and 500uL of NaAc 3M and 5 mL of isopropanol was added then incubation over night at RT and followed by a centrifuge 30 mins/20°C/12000g. Pellet was washed using EtOH and dissolve in H2O.

Illumina P5 and P7-barcoded adaptors were added by PCR on gDNA samples according to the GoTaq protocol (Promega). PCR amplicons were gel purified and sequenced on a HiSeq4000 (Illumina). Enrichment of gRNAs was analysed using MaGeCK with default parameters (Li et al., 2014). Primers used to generate the PCR products are listed in Table S1. The results of the dsRNA and SINV screen are available in Dataset S1 and S2, respectively

Generation of monoclonal SLC35B2 and B4GALT7 knock-out HCT116 cell lines.

The gRNA expression vectors targeting either SLC35B2 or B4GALT7 (gRNA sequences selected were the 2 most enriched gRNA in the dsRNA screen) genes were produced by annealing the "sense" and "antisense" oligonucleotides (Table S1) at a concentration of 10 µM in 10 mM Tris-HCl (pH 8.0), 50 mM MgCl2 in 100 μL. The mixture was incubated at 95 ° C for 5 minutes and then allowed to cool down to room temperature. The oligonucleotide duplex thus formed was cloned into the BbsI restriction site of the plasmid pKLV-U6gRNA (BbsI)-

pGKpuro2ABFP (Addgene#62348). The lentiviral supernatant from single transfer vector was produced by transfecting HEK293T cells (ATCC® CRL-3216™) with the transfer vector, psPAX2 packaging plasmid (Addgene #12260) and the pVSV envelope plasmid (Addgene #8454) in proportion 5:4:1 using Lipofectamine™ 2000 (Themofisher) reagent according to manufacturer protocol. Standard DMEM (GIBCO) medium supplemented with 10% Fetal bovine serum (FBS, Gibco) and 100 U/mL of penicillin-Streptomycin (Gibco) was used for growing HEK293T cells and for lentivirus production. One 10 cm plate of HEK293T cells at 70-80% confluency was used for the transfection. The medium was replaced 8 hours post-transfection. After 48 hours the medium containing viral particles was collected and filtered through a 0.45μm PES filter. The supernatant was directly used for transfection or stored at -80°C. A 6 well plate of HCT116cas9 cells at 80% confluency was transduced using 600 μL of lentiviral supernatant (300 μL of each lentivirus produced for each duplexes) supplemented with 4 ug/mL polybrene (Sigma) for 6 hours. The transduction media was then changed with fresh DMEM for 24 hours then the transduced cells were selected using DMEM containing 10 μg/mL Blasticidin (Invivogen) and 1 μg/mL Puromycin (Invivogen). Genomic DNA was isolated from individual colonies and KO clones were screened by PCR (primers in Table S1). The expected WT band for SLC35B2 is 469 bp and the mutant band 132 bp. For B4GALT7, the WT band is 341 bp and mutant band 180 bp. For laboratory purposes, the SLC35B2 clones have been generated into HCT116cas9 cells that are expressing mCherry and Citrine due to integration of miReporter-PGK (Addgene#82477).

Nucleic acids delivery

Transfection using lipofectamine2000 (InvitroGen – 11668019) were performed following manufacturer's instructions. For nucleofection, cells were nucleofected using Nucleofector SE solution and reagent into Nucleocuvette following manufacturer's instructions using 4D-

Nucleofector System (Lonza). The cell number and nucleic acid amounts are indicated in each figure legends. P-EGFP-N1 (Addgene plasmid#2491) was used in transfection and nucleofection experiments as a control.

Viability assay

PrestoBlue (PB) reagent (ThermoFisher – A13261) was used for viability assay according to the manufacturer's protocol. After 24 to 48 hours post treatment (dsRNA transfection/nucleofection), cells were incubated with PB reagent and cell viability was assessed by measuring the fluorescence (excitation 570 nm; emission 590 nm) after 20 mins incubation using SAFAS spectrofluorometer (Xenius XC).Cell viability was expressed as a percentage relative to untreated cells.

Heparinase & sodium chlorate treatment and heparan sulfate staining

Heparinase: 1*10^6 cells were treated with 2U of Heparinase I and III blend from *Flavobacterium heparinum* (Merck – H3917) for 1 h at 37°C 5% CO2 in DMEM and then cells were reverse transfected with 2 µg of GFP using lipofectamine2000 (Invitrogen) in 6 well plate.

Sodium chlorate: HCT116cas9 cells grow in 50 mM sodium chlorate (Merck – 1.06420) DMEM 10 % FBS for at least 48 h then 150 000 cells were reverse transfected with 500 ng of GFP using lipofectamine 2000 (Invitrogen) in 24 well plate.

24 (heparinase) or 48 (sodium chlorate) hours post treatment, cells were detach using PBS 0.02% EDTA then heparan sulfate of the cells were stained using 1:30 of F58-10E4 as primary antibody (AMSBIO, cat#370255-S) in PBS 3% BSA for 30 to 40 minutes on ice then washed with PBS 1% FBS and incubated with 1:30 anti-mouse Alexa Fluor 594 (Thermo, A-11032) in PBS 3% BSA, washed twice using PBS 1% FBS then and analysed at FACS using FACS Calibur.

dsRNA preparation

PCR fragments corresponding to 231 nts of the Citrine coding sequence were amplified from ES-FUCCI plasmid (Addgene plasmid#62451) using primers containing T7 promoter sequence with 2 distinct PCR fragment allowing the positive-sense or negative-sense RNA. Primers used to generate the PCR products are listed in Table S1. The PCR fragments were produced using DyNAzyme EXT DNA Polymerase (F-505S - Thermo Scientific) and purified using Monarch DNA extraction (T1020L - New England Biolab). In vitro transcription (IVT) with homemade T7 RNA polymerase was performed for 4 hours at 37°C. To label the IVT RNA, 1/10th of Cy5-CTP (Amersham CyDye Fluorescent Nucleotides Cy5-CTP, GE Healthcare Life sciences) was included in the IVT reaction. IVT RNA was digested with DNase I (EN0525 - Thermo Scientific) for 30 min at 37°C and IVT product was purified, unincorporated nucleotides removed and size checked using UV shadow (8% acrylamide-urea gel) followed by phenol-chloroform extraction the nanodrop quantification for each strand. We then mix an equal quantity of positive-strand and negative-strand RNA, heat for 5' at 95°C followed by slow cool down to RT. The integrity of dsRNA is then checked by RNases T1 (EN0541 - Thermo Scientific) and V1 (AM2275, Ambion) digestion.

Microscopy

Imaging of cells treated with dsRNA/GFP plasmid was carried out on the Observer A1 (Zeiss) microscope and analyzed using Fiji (Schindelin et al., 2012). Images of cells transfected with Poly(I:C) (LMW) Rhodamine (tlrl-piwr – Invivogen)(1,8 ug/mL, 24h post plating of 76 000 cells) into Lab-Tek on glass coverslip (155411- Thermo Scientific) were acquired using a 100x Plan Apochromat oil immersion NA1.4 objective on a spinning disk system Axio Observer Z1 (Zeiss) every 20 minutes for 72 hours. All pictures were acquired under the same conditions

(laser power and amplification gain) then processed with Fiji. Images of cells infected with SINV stained with J2 antibody were carried out on the BX51 (Olympus).

FACS analysis

The cells intended for analysis by flow cytometry are recovered mechanically (PBS 0,5 mM EDTA) or using trypsin, washed in PBS and then suspended in PBS 1 % FBS. Each acquisition includes at least 10,000 events and is performed on the FACScalibur (BD Bioscience) device. The data produced is processed using FlowJo software (FlowJo LLC).

RT-qPCR analysis

Total RNA was isolated using TRIzol (Invitrogen - 15596026) following manufacturer's instructions. 1 µg of RNA was reverse transcribed using SuperScript IV Vilo (Invitrogen – 11756050) according to manufacturer's instructions. Real-time PCR was performed using SYBR Green (Applied Biosystem – 4309155) and primers listed in Table S1 at an annealing temperature of 60°C on a CFX96 thermal cycler (Biorad). Generated data were analysed using the CFX Manager Software (Biorad).

Western blot analysis

Proteins were extracted using TRIzol (Invitrogen – 15596026) then precipitate using 3 volumes of 100% acetone and washed with 70% acetone and resuspended in 3% SDS, 62.3 mM Tris-HCL pH 8 10% glycerol . Proteins were quantified by the Bradford method and 20 to 30 µg of total protein extract was loaded on 4-20% Mini-PROTEAN® TGX™ Precast Gels (Biorad). After transfer onto nitrocellulose membrane, equal loading was verified by Ponceau staining. Membranes were blocked in 5% milk and probed with the following antibodies: anti-COG4 (1:300, from V. Lupashin), anti-p-eIF2a (1/1000, Ser-52 Santa Cruz sc-601670), and anti-

gamma-Tubulin (1:10000, Sigma T6557). Detection was performed using Chemiluminescent Substrate (Thermo Fisher).

Acknowledgments

The authors would like to thank members of the Pfeffer laboratory for discussion, Delphine Richer for technical help, Dr. Jean-Daniel Fauny for help with the spinning disk microscope and Dr. Frédéric Gros for help with FACS analysis, Dr Carla Saleh for providing us the SINV WT and GFP clones.

This work was funded by the European Research Council (ERC-CoG-647455 RegulRNA) and was performed under the framework of the LABEX: ANR-10-LABX-0036_NETRNA, which benefits from a funding from the state managed by the French National Research Agency as part of the Investments for the future program. This work has also received funding from the People Programme (Marie Curie Actions) of the European Union's Seventh Framework Program (FP7/2007-2013) under REA grant agreement n° PCOFUND-GA-2013-609102, through the PRESTIGE program coordinated by Campus France (to EG), and from the French Minister for Higher Education, Research and Innovation (PhD contract to OP) . VL was supported by the National Institutes of Health (R01GM083144).

Authors contribution

SP and EG conceived the project. SP, EG and OP designed the work and analysed the results. OP, EG, and RPN performed the experiments. EG and OP set up the CRISPR/Cas9 screens, RPN generated the lentivirus library and the HCT16-Cas9 cell line. OP and RPN performed the bioinformatics analysis of the screens. OP generated the SLC35B2 and B4GALT7 KO clones. OP generated IVT dsRNA and perform validation of cell survival. EG produced SINV-GFP viral stock, performed the infections and analysed viral titers. OP performed FACS analyses.

EG and OP performed the immunofluorescence assays. OP analysed the live-imaging microscopy data. VL provided the COG KO cells and antibodies. OP, EG and SP wrote the manuscript with input from the other authors. SP and EG coordinated the work. SP assured funding. All authors reviewed the final manuscript.

References

Bailey Blackburn, J., I. Pokrovskaya, P. Fisher, D. Ungar, and V.V. Lupashin. 2016. COG Complex Complexities: Detailed Characterization of a Complete Set of HEK293T Cells Lacking Individual COG Subunits. *Front. Cell Dev. Biol.* 4. doi:10.3389/fcell.2016.00023.

Bishop, J.R., M. Schuksz, and J.D. Esko. 2007. Heparan sulphate proteoglycans fine-tune mammalian physiology. *Nature*. 446:1030–1037. doi:10.1038/nature05817.

Blackburn, J.B., Z. D'Souza, and V.V. Lupashin. 2019. Maintaining order: COG complex controls Golgi trafficking, processing, and sorting. *FEBS Lett.* 593:2466–2487. doi:10.1002/1873-3468.13570.

Blackburn, J.B., T. Kudlyk, I. Pokrovskaya, and V.V. Lupashin. 2018a. More than just sugars: Conserved oligomeric Golgi complex deficiency causes glycosylation-independent cellular defects. *Traffic*. 19:463–480. doi:10.1111/tra.12564.

Blackburn, J.B., T. Kudlyk, I. Pokrovskaya, and V.V. Lupashin. 2018b. More than just sugars: Conserved oligomeric Golgi complex deficiency causes glycosylation-independent cellular defects. *Traffic*. 19:463–480. doi:10.1111/tra.12564.

Blackburn, J.B., and V.V. Lupashin. 2016. Creating Knockouts of Conserved Oligomeric Golgi Complex Subunits Using CRISPR-Mediated Gene Editing Paired with a Selection Strategy Based on Glycosylation Defects Associated with Impaired COG Complex Function. *In* The Golgi Complex. W.J. Brown, editor. Springer New York, New York, NY. 145–161.

Bomsel, M., and A. Alfsen. 2003. Entry of viruses through the epithelial barrier: pathogenic trickery. *Nat. Rev. Mol. Cell Biol.* 4:57–68. doi:10.1038/nrm1005.

Byrnes, A.P., and D.E. Griffin. 1998. Binding of Sindbis Virus to Cell Surface Heparan Sulfate. *J. VIROL.* 72:8.

Cagno, V., E.D. Tseligka, S.T. Jones, and C. Tapparel. 2019. Heparan Sulfate Proteoglycans and Viral Attachment: True Receptors or Adaptation Bias? *Viruses*. 11. doi:10.3390/v11070596.

Climer, L.K., I.D. Pokrovskaya, J.B. Blackburn, and V.V. Lupashin. 2018. Membrane detachment is not essential for COG complex function. *MBoC*. 29:964–974. doi:10.1091/mbc.E17-11-0694.

Doench, J.G., N. Fusi, M. Sullender, M. Hegde, E.W. Vaimberg, K.F. Donovan, I. Smith, Z. Tothova, C. Wilen, R. Orchard, H.W. Virgin, J. Listgarten, and D.E. Root. 2016. Optimized sgRNA design to maximize activity and minimize off-target effects of CRISPR-Cas9. *Nat Biotechnol*. 34:184–191. doi:10.1038/nbt.3437.

D'Souza, Z., J.B. Blackburn, T. Kudlyk, I.D. Pokrovskaya, and V.V. Lupashin. 2019. Defects in COG-Mediated Golgi Trafficking Alter Endo-Lysosomal System in Human Cells. *Front. Cell Dev. Biol.* 7:118. doi:10.3389/fcell.2019.00118.

García, M.A., E.F. Meurs, and M. Esteban. 2007. The dsRNA protein kinase PKR: Virus and cell control. *Biochimie*. 89:799–811. doi:10.1016/j.biochi.2007.03.001.

Golden, R.J., B. Chen, T. Li, J. Braun, H. Manjunath, X. Chen, J. Wu, V. Schmid, T.-C. Chang, F. Kopp, A. Ramirez-Martinez, V.S. Tagliabracci, Z.J. Chen, Y. Xie, and J.T. Mendell. 2017. An Argonaute phosphorylation cycle promotes microRNA-mediated silencing. *Nature*. 542:197–202. doi:10.1038/nature21025.

Han, J., J.T. Perez, C. Chen, Y. Li, A. Benitez, M. Kandasamy, Y. Lee, J. Andrade, B. tenOever, and B. Manicassamy. 2018. Genome-wide CRISPR/Cas9 Screen Identifies Host Factors Essential for Influenza Virus Replication. *Cell Reports*. 23:596–607. doi:10.1016/j.celrep.2018.03.045.

Jae, L.T., M. Raaben, M. Riemersma, E. van Beusekom, V.A. Blomen, A. Velds, R.M. Kerkhoven, J.E. Carette, H. Topaloglu, P. Meinecke, M.W. Wessels, D.J. Lefeber, S.P. Whelan, H. van Bokhoven, and T.R. Brummelkamp. 2013. Deciphering the Glycosylome of Dystroglycanopathies Using Haploid Screens for Lassa Virus Entry. *Science*. 340:479–483. doi:10.1126/science.1233675.

Klimstra, W.B., K.D. Ryman, and R.E. Johnston. 1998. Adaptation of Sindbis Virus to BHK Cells Selects for Use of Heparan Sulfate as an Attachment Receptor. *Journal of Virology*. 72:7357–7366. doi:10.1128/JVI.72.9.7357-7366.1998.

Kranz, C., B.G. Ng, L. Sun, V. Sharma, E.A. Eklund, Y. Miura, D. Ungar, V. Lupashin, R.D. Winkel, J.F. Cipollo, C.E. Costello, E. Loh, W. Hong, and H.H. Freeze. 2007. COG8 deficiency causes new congenital disorder of glycosylation type IIh. *Human Molecular Genetics*. 16:731–741. doi:10.1093/hmg/ddm028.

Li, J.-P., and M. Kusche-Gullberg. 2016. Heparan Sulfate: Biosynthesis, Structure, and Function. *In* International Review of Cell and Molecular Biology. Elsevier. 215–273.

Li, W., H. Xu, T. Xiao, L. Cong, M.I. Love, F. Zhang, R.A. Irizarry, J.S. Liu, M. Brown, and X.S. Liu. 2014. MAGeCK enables robust identification of essential genes from genome-scale CRISPR/Cas9 knockout screens. *Genome Biol*. 15:554. doi:10.1186/s13059-014-0554-4.

Li, Y., J. Muffat, A. Omer Javed, H.R. Keys, T. Lungjangwa, I. Bosch, M. Khan, M.C. Virgilio, L. Gehrke, D.M. Sabatini, and R. Jaenisch. 2019. Genome-wide CRISPR screen for Zika virus resistance in human neural cells. *Proc Natl Acad Sci USA*. 201900867. doi:10.1073/pnas.1900867116.

Lindahl, U., J. Couchman, K. Kimata, and J.D. Esko. 2015. Proteoglycans and Sulfated Glycosaminoglycans. *In* Essentials of Glycobiology. A. Varki, R.D. Cummings, J.D. Esko, P. Stanley, G.W. Hart, M. Aebi, A.G. Darvill, T. Kinoshita, N.H. Packer, J.H. Prestegard, R.L. Schnaar, and P.H. Seeberger, editors. Cold Spring Harbor Laboratory Press, Cold Spring Harbor (NY).

López, P., E. Girardi, B.C. Mounce, A. Weiss, B. Chane-Woon-Ming, M. Messmer, P. Kaukinen, A. Kopp, D. Bortolamiol-Becet, A. Fendri, M. Vignuzzi, L. Brino, and S. Pfeffer. 2020. High-throughput fluorescence-based screen identifies the neuronal

microRNA miR-124 as a positive regulator of alphavirus infection. *J Virol*. JVI.02145-19, jvi;JVI.02145-19v1. doi:10.1128/JVI.02145-19.

Mislick, K.A., and J.D. Baldeschwieler. 1996. Evidence for the role of proteoglycans in cation-mediated gene transfer. *Proceedings of the National Academy of Sciences*. 93:12349–12354. doi:10.1073/pnas.93.22.12349.

Murakami, S., A. Takenaka-Uema, T. Kobayashi, K. Kato, M. Shimojima, M. Palmarini, and T. Horimoto. 2017. Heparan Sulfate Proteoglycan Is an Important Attachment Factor for Cell Entry of Akabane and Schmallenberg Viruses. *J. Virol*. 91:e00503-17, /jvi/91/15/e00503-17.atom. doi:10.1128/JVI.00503-17.

Park, R.J., T. Wang, D. Koundakjian, J.F. Hultquist, P. Lamothe-Molina, B. Monel, K. Schumann, H. Yu, K.M. Krupzcak, W. Garcia-Beltran, A. Piechocka-Trocha, N.J. Krogan, A. Marson, D.M. Sabatini, E.S. Lander, N. Hacohen, and B.D. Walker. 2017. A genome-wide CRISPR screen identifies a restricted set of HIV host dependency factors. *Nat. Genet*. 49:193–203. doi:10.1038/ng.3741.

Payne, C.K., S.A. Jones, C. Chen, and X. Zhuang. 2007. Internalization and Trafficking of Cell Surface Proteoglycans and Proteoglycan-Binding Ligands. *Traffic*. 8:389–401. doi:10.1111/j.1600-0854.2007.00540.x.

Reynders, E., F. Foulquier, E. Leão Teles, D. Quelhas, W. Morelle, C. Rabouille, W. Annaert, and G. Matthijs. 2009a. Golgi function and dysfunction in the first COG4-deficient CDG type II patient. *Human Molecular Genetics*. 18:3244–3256. doi:10.1093/hmg/ddp262.

Reynders, E., F. Foulquier, E. Leão Teles, D. Quelhas, W. Morelle, C. Rabouille, W. Annaert, and G. Matthijs. 2009b. Golgi function and dysfunction in the first COG4-deficient CDG type II patient. *Human Molecular Genetics*. 18:3244–3256. doi:10.1093/hmg/ddp262.

Rusnati, M., E. Vicenzi, M. Donalisio, P. Oreste, S. Landolfo, and D. Lembo. 2009. Sulfated K5 Escherichia coli polysaccharide derivatives: A novel class of candidate antiviral microbicides. *Pharmacology & Therapeutics*. 123:310–322. doi:10.1016/j.pharmthera.2009.05.001.

Safaiyan, F., S.O. Kolset, K. Prydz, E. Gottfridsson, U. Lindahl, and M. Salmivirta. 1999. Selective Effects of Sodium Chlorate Treatment on the Sulfation of Heparan Sulfate. *J. Biol. Chem*. 274:36267–36273. doi:10.1074/jbc.274.51.36267.

Savidis, G., W.M. McDougall, P. Meraner, J.M. Perreira, J.M. Portmann, G. Trincucci, S.P. John, A.M. Aker, N. Renzette, D.R. Robbins, Z. Guo, S. Green, T.F. Kowalik, and A.L. Brass. 2016. Identification of Zika Virus and Dengue Virus Dependency Factors using Functional Genomics. *Cell Reports*. 16:232–246. doi:10.1016/j.celrep.2016.06.028.

Schindelin, J., I. Arganda-Carreras, E. Frise, V. Kaynig, M. Longair, T. Pietzsch, S. Preibisch, C. Rueden, S. Saalfeld, B. Schmid, J.-Y. Tinevez, D.J. White, V. Hartenstein, K. Eliceiri, P. Tomancak, and A. Cardona. 2012. Fiji: an open-source platform for biological-image analysis. *Nat Methods*. 9:676–682. doi:10.1038/nmeth.2019.

Schlee, M., and G. Hartmann. 2016. Discriminating self from non-self in nucleic acid sensing. *Nat Rev Immunol*. 16:566–580. doi:10.1038/nri.2016.78.

Shalem, O., N.E. Sanjana, and F. Zhang. 2015. High-throughput functional genomics using CRISPR-Cas9. *Nat. Rev. Genet*. 16:299–311. doi:10.1038/nrg3899.

Shestakova, A., S. Zolov, and V. Lupashin. 2006. COG Complex-Mediated Recycling of Golgi Glycosyltransferases is Essential for Normal Protein Glycosylation: COG Complex and Golgi Glycosylation. *Traffic*. 7:191–204. doi:10.1111/j.1600-0854.2005.00376.x.

Sievers, F., A. Wilm, D. Dineen, T.J. Gibson, K. Karplus, W. Li, R. Lopez, H. McWilliam, M. Remmert, J. Söding, J.D. Thompson, and D.G. Higgins. 2011. Fast, scalable generation of high-quality protein multiple sequence alignments using Clustal Omega. *Mol Syst Biol*. 7:539. doi:10.1038/msb.2011.75.

Smith, T.J., R.H. Cheng, N.H. Olson, P. Peterson, E. Chase, R.J. Kuhn, and T.S. Baker. 1995. Putative receptor binding sites on alphaviruses as visualized by cryoelectron microscopy. *Proceedings of the National Academy of Sciences*. 92:10648–10652. doi:10.1073/pnas.92.23.10648.

Spaapen, L.J.M., J.A. Bakker, S.B. van der Meer, H.J. Sijstermans, R.A. Steet, R.A. Wevers, and J. Jaeken. 2005. Clinical and biochemical presentation of siblings with COG-7 deficiency, a lethal multiple O- and N-glycosylation disorder. *J Inherit Metab Dis*. 28:707–714. doi:10.1007/s10545-005-0015-z.

Stetson, D.B., and R. Medzhitov. 2006. Type I Interferons in Host Defense. *Immunity*. 25:373–381. doi:10.1016/j.immuni.2006.08.007.

Strauss, J.H., and E.G. Strauss. 1994. The alphaviruses: gene expression, replication, and evolution. *Microbiol. Rev*. 58:491–562.

Tanaka, A., U. Tumkosit, S. Nakamura, D. Motooka, N. Kishishita, T. Priengprom, A. Sangasang, T. Kinoshita, N. Takeda, and Y. Maeda. 2017. Genome-Wide Screening Uncovers the Significance of N-Sulfation of Heparan Sulfate as a Host Cell Factor for Chikungunya Virus Infection. *J. Virol*. 91:e00432-17, /jvi/91/13/e00432-17.atom. doi:10.1128/JVI.00432-17.

Ungar, D., T. Oka, E.E. Brittle, E. Vasile, V.V. Lupashin, J.E. Chatterton, J.E. Heuser, M. Krieger, and M.G. Waters. 2002. Characterization of a mammalian Golgi-localized protein complex, COG, that is required for normal Golgi morphology and function. *The Journal of Cell Biology*. 157:405–415. doi:10.1083/jcb.200202016.

Wahlberg, J.M., R. Bron, J. Wilschut, and H. Garoff. 1992. Membrane fusion of Semliki Forest virus involves homotrimers of the fusion protein. *J. Virol*. 66:7309–7318.

Weber, F., V. Wagner, S.B. Rasmussen, R. Hartmann, and S.R. Paludan. 2006. Double-Stranded RNA Is Produced by Positive-Strand RNA Viruses and DNA Viruses but Not in Detectable Amounts by Negative-Strand RNA Viruses. *Journal of Virology*. 80:5059–5064. doi:10.1128/JVI.80.10.5059-5064.2006.

Willett, R., D. Ungar, and V. Lupashin. 2013. The Golgi puppet master: COG complex at center stage of membrane trafficking interactions. *Histochem Cell Biol*. 140:271–283. doi:10.1007/s00418-013-1117-6.

Zeevaert, R., F. Foulquier, J. Jaeken, and G. Matthijs. 2008. Deficiencies in subunits of the Conserved Oligomeric Golgi (COG) complex define a novel group of Congenital Disorders of Glycosylation. *Molecular Genetics and Metabolism*. 93:15–21. doi:10.1016/j.ymgme.2007.08.118.

Zhang, R., J.J. Miner, M.J. Gorman, K. Rausch, H. Ramage, J.P. White, A. Zuiani, P. Zhang, E. Fernandez, Q. Zhang, K.A. Dowd, T.C. Pierson, S. Cherry, and M.S. Diamond. 2016. A CRISPR screen defines a signal peptide processing pathway required by flaviviruses. *Nature*. 535:164–168. doi:10.1038/nature18625.

Zolov, S.N., and V.V. Lupashin. 2005. Cog3p depletion blocks vesicle-mediated Golgi retrograde trafficking in HeLa cells. *J Cell Biol*. 168:747–759. doi:10.1083/jcb.200412003.

Figures legends

Figure 1. CRISPR-Cas9 screen for dsRNA resistance factors identifies the extracellular heparan-sulfates as necessary for nucleic acids internalization.

A. Schematic representation of the CRISPR-Cas9 approach. HCT116 cells expressing Cas9 were transduced with the lentiviral gRNA library Brunello (MOI 0.3). Transduced cells were selected with 1 μg/mL puromycin to generate a mutant cell population. Selective pressure (1 μg/mL synthetic dsRNA) was applied to induce cell death. Genomic DNA of input and cells surviving to the dsRNA treatment were extracted and CRISPR-Cas9 guides sequenced on an Illumina HiSeq400 sequencer. The data produced was processed by MAGeCK. Three independent experiments were performed. **B.** Bubble plot of candidate genes. Significance of RRA score is calculated for each gene in dsRNA treated cells condition compared to INPUT cells using MAGeCK analysis. The number of enriched gRNAs is represented by the size of the bubble and pathways associated with the top hits are indicated in blue and green. **C.** Viability assay. Cells were transfected (80 000 cells; 1 μg/mL) or nucleofected (200 000 cells; 400 ng) with dsRNA and cell viability was quantified 24 h (nucleofection) or 48 h (transfection) post treatment using PrestoBlue reagent. Average of at least three independent biological experiments +/- SD is shown. One-way ANOVA analysis, * $p < 0.05$. **D.** Representative pictures of transfectability assay. Cells were transfected (80 000 cells; 2 μg/mL) or nucleofected (200 000 cells; 500 ng) with a plasmid coding for GFP and the GFP positive cells were observed by fluorescence microscopy at 24 h (nucleofection) or 48 h (transfection) post treatment. Pictures were taken at 10× magnification, scale bar represents 50 μm. One representative experiment out of three is shown. **E.** Representative quantification of extracellular heparan-sulfates. FACS analysis of HCT116 control or KO clones stained with the HS-specific antibody 10E4 (in red) compared to unstained samples (in blue). One representative experiment out of three is shown. **F and G.** Transfectability assay upon heparan-sulfates depletion. Cells were

treated with 50 mM sodium chlorate (F) or with 2 units of heparinase (G) then transfected with GFP plasmid. GFP intensity of fluorescence was quantified 48 h post transfection using FACS. Data from four independent biological experiments +/- SD are shown. Unpaired t.test analysis, * $p < 0.05$.

Figure 2. COG4 is a novel dsRNA resistance factor.

A. Viability assay. Cells (80 000 cells; 1 µg/mL) were transfected with dsRNA then the viability of the cells was quantified 48 h post transfection using PrestoBlue reagent. Data from at least three independent biological experiments are shown.One-way ANOVA analysis, * $p < 0.05$. **B.** Representative quantification of extracellular heparan-sulfates. FACS analysis of HEK293T (in red), COG4 KO (in blue) and rescued cells (in orange) stained with the HS-specific antibody 10E4. One representative experiment out of three is shown. **C.** Representative pictures of transfectability assay. Cells were transfected (80 000 cells; 2 µg/mL) with plasmid coding for GFP and the GFP positive cells were observed by fluorescence microscopy 48 h post treatment. Pictures were taken at 10× magnification, scale bar represent 50 µm. One representative experiment out of four is shown. **D.** qPCR quantification. Cells (300 000 cells; 1 µg/mL) were transfected with dsRNA and total RNA was extracted 24 h post transfection and quantified using RT-qPCR. The histogram represents the expression fold change of dsRNA relative to GAPDH into dsRNA transfected HEK293T KO COG4 rescued compared to HEK293T KO COG4. Average of three independent biological experiments +/- SD are shown. Unpaired t.test analysis * $p < 0.05$. **E.** Confocal microscopy. Cells transfected with synthetic dsRNA for 24 hours were fixed and stained with DAPI and J2 antibody (anti-dsRNA). Pictures were taken at 100× magnification using a spinning-disk confocal microscope. **F.** Western Blot. Cells (300 000 cells; 1 µg/mL) were transfected with dsRNA then proteins were extracted 24 h post transfection and analysed by Western Blot. Antibody against COG4 and p-EIF2alpha were

used. * corresponds to an aspecific band. Gamma-tubulin was used as loading control. One representative experiment out of three is shown.

Figure 3. CRISPR-Cas9 screen identifies *COG4* as a permissivity factor to SINV

A. Schematic representation of the CRISPR-Cas9 approach. HCT116 cells expressing Cas9 were transduced with the lentiviral gRNA library Brunello (MOI 0.3). Transduced cells were selected with 1 μg/mL puromycin to generate a mutant cell population. Selective pressure (SINV MOI 0,1) was applied to induce cell death. Genomic DNA of input and cells surviving the SINV infection were extracted and sequenced on an Illumina HiSeq400 sequencer. Three independent experiments were performed. The data produced was processed by MAGeCK. **B.** Bubble plot of candidate genes. Significance of RRA score is calculated for each gene in SINV infected cells compared to INPUT cells using MAGeCK analysis. The number of enriched gRNAs is underlined by the size of the bubble and pathways associated with the top hits are indicated. **C.** SINV infection. Cells were infected with SINV encoding for GFP at MOI of 0.1 and the GFP positive cells were observed by fluorescence microscopy at 24 h and 48 h post infection. Representative pictures were taken at 20x magnification One representative experiment out of three is shown. **D.** Plaque assay. WT, COG4KO and rescued HEK293T cells were infected with SINV-GFP for 24 h at MOI of 1 and supernatant was collected in order to measure viral production. The fold change in titer relative to HEK293T arbitrarily set to 1 is shown. Average of three independent biological experiments +/- SD is shown. ANOVA analysis * $p < 0.05$. **E.** Immunofluorescence assay. Cells were infected with SINV for 24 h at MOI of 0.1 for 24 h then fixed and stained with J2 antibody and DAPI. Pictures were taken at 40× magnification with BX51 (Olympus) microscope.

Supplemental information

Supplemental figures legends

Figure S1. HCT116 cells are infectable by SINV and are sensitive to dsRNA-induced cell death.

A. Representative pictures of HCT116cas9 cells uninfected or infected with SINV-GFP MOI of 1at 24h post infection. 20X optical microscopy**. B.** Representative pictures of HCT116cas9 cells at 48h post transfection with 1 ug/mL dsRNA compared to non transfected ones. 10X optical microscopy.

Figure S2. Generation of SLC35B2 and B4GALT7 HCT116 CRISPR/Cas9 knock-out monoclonal cell lines.

A. PCR screen of SLC35B2 and B4GALT7 knock-out clones obtained by CRISPR/Cas9. The gels show the amplicons corresponding to wild type and deleted alleles that were subsequently sequenced. **B.** Clustal Omega (Sievers et al., 2011) alignment of the wild type and mutated peptide sequences corresponding to the genomic deletions identified in the different clones. The reference aminoacidic sequence is represented in yellow (unknown domains - InterPro) and orange (known domains – InterPro). The peptidic sequences resulting in shorter protein due to deletions or formation of premature stop codon in the knock-out clones are represented with black bars or red rectangles, respectively.

Figure S3. DsRNA delivery is impaired in the absence of extracellular heparan-sulfates.

A. Cy5-labeled dsRNA (1 µg/mL) was transfected into HCT116cas9, B4GALT7#1 and 2, SLC35B2#1 and #2 cells and Cy5 fluorescence was quantified using FACSCalibur (10 000 events). Average of three independent biological experiments +/- SD are shown. One-way

ANOVA analysis, * $p < 0.05$. **B and C.** HCT116cas9 cells were treated with (**B**) 50 mM sodium chlorate or (**C**) 2 units of heparinase before transfection of a GFP plasmid. HS were stained 48h post transfection using 10E4 antibody and quantified using FACSCalibur (10 000 events). Data from at least three independent biological experiments +/- SD are shown Unpaired t.test analysis * $p < 0.05$.

Figure S4. Plasmid DNA and dsRNA are differentially internalized in HEK293T *COG4* KO cells.

A. HEK293T and HEK293T KO *COG4* cells were transfected with a GFP plasmid and fluorescence was quantified 48h post transfection using FACSCalibur. Average of three experiments +/- SD are shown. Unpaired t.test analysis * $p < 0.05$.

B. Cy5-labeled dsRNA (1 µg/mL was transfected into HEK293T, HEK293T KO *COG4* cells and HEK293T KO *COG4* rescued cells. Cy5 fluorescence was quantified using FACSCalibur (10 000 events). Average of three experiments +/- SD are shown.. One-way ANOVA analysis, * $p < 0.05$. **C.** HEK293T and HEK293T KO *COG4* were transfected with rhodamine-labeled poly I:C (in red) and with Rab5-GFP (in green) and images were acquired using spinning disk microscope. Representative pictures are shown. **D**. The approximative number of rhodamine-positive signal of per cells was quantified by counting 7 fields per conditions. Two-way ANOVA analysis, * $p < 0.05$.

Table S1

List of primers used in the study.

Dataset S1

MAGeCK comparison report dsRNA versus Input

Dataset S2

MAGeCK comparison report SINV versus Input

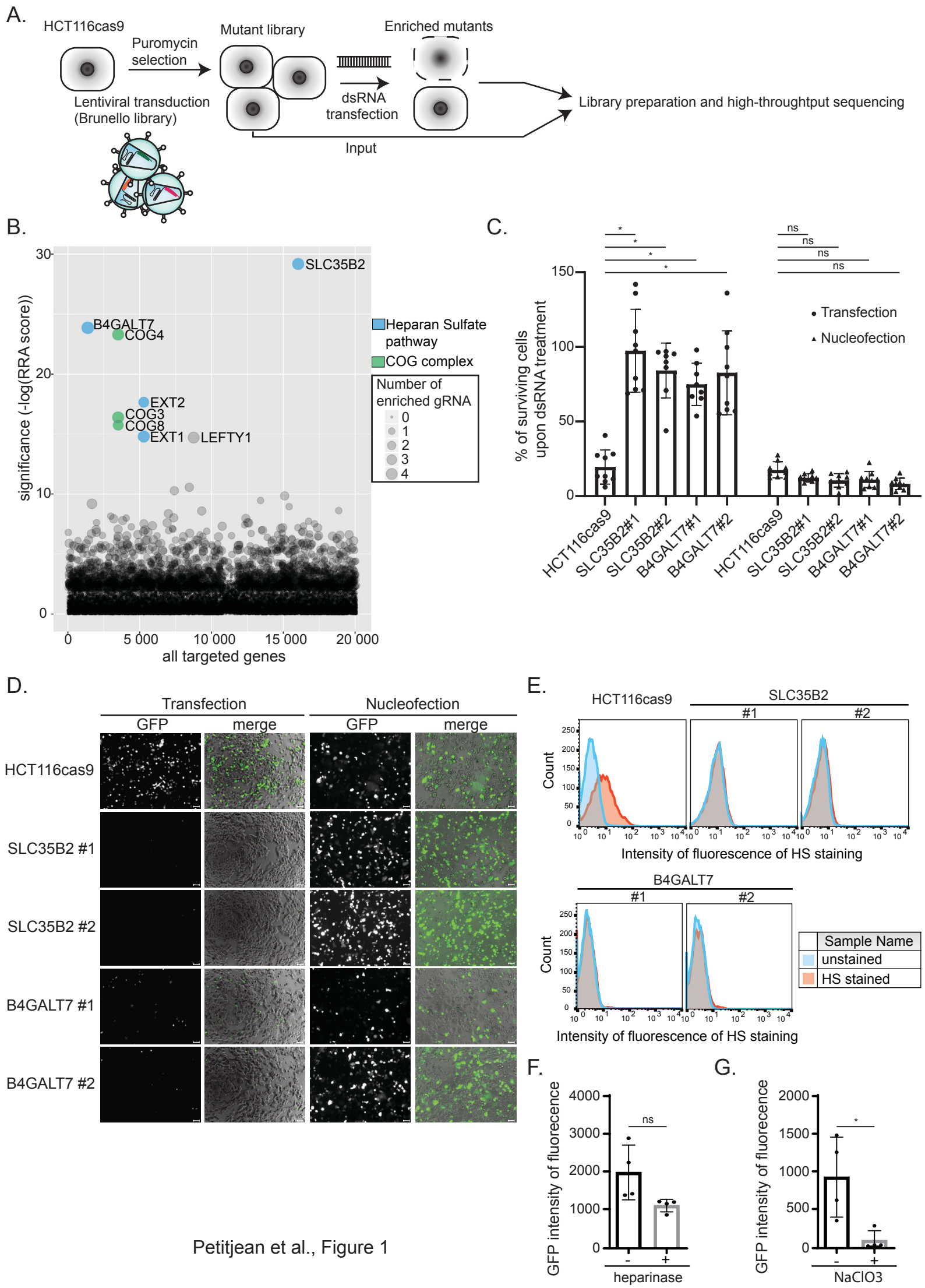

Petitjean et al., Figure 1

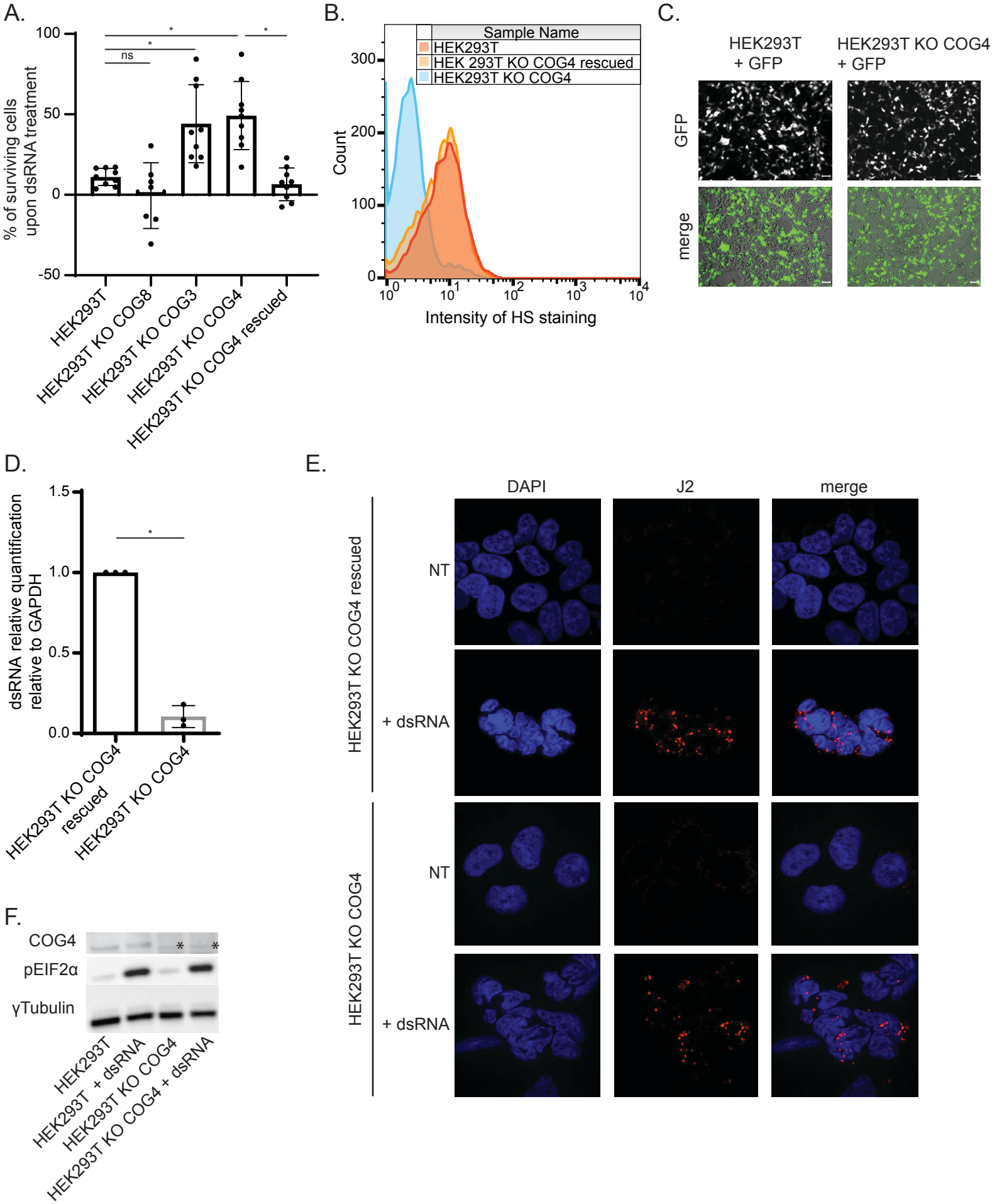

Petitjean et al., Figure 2

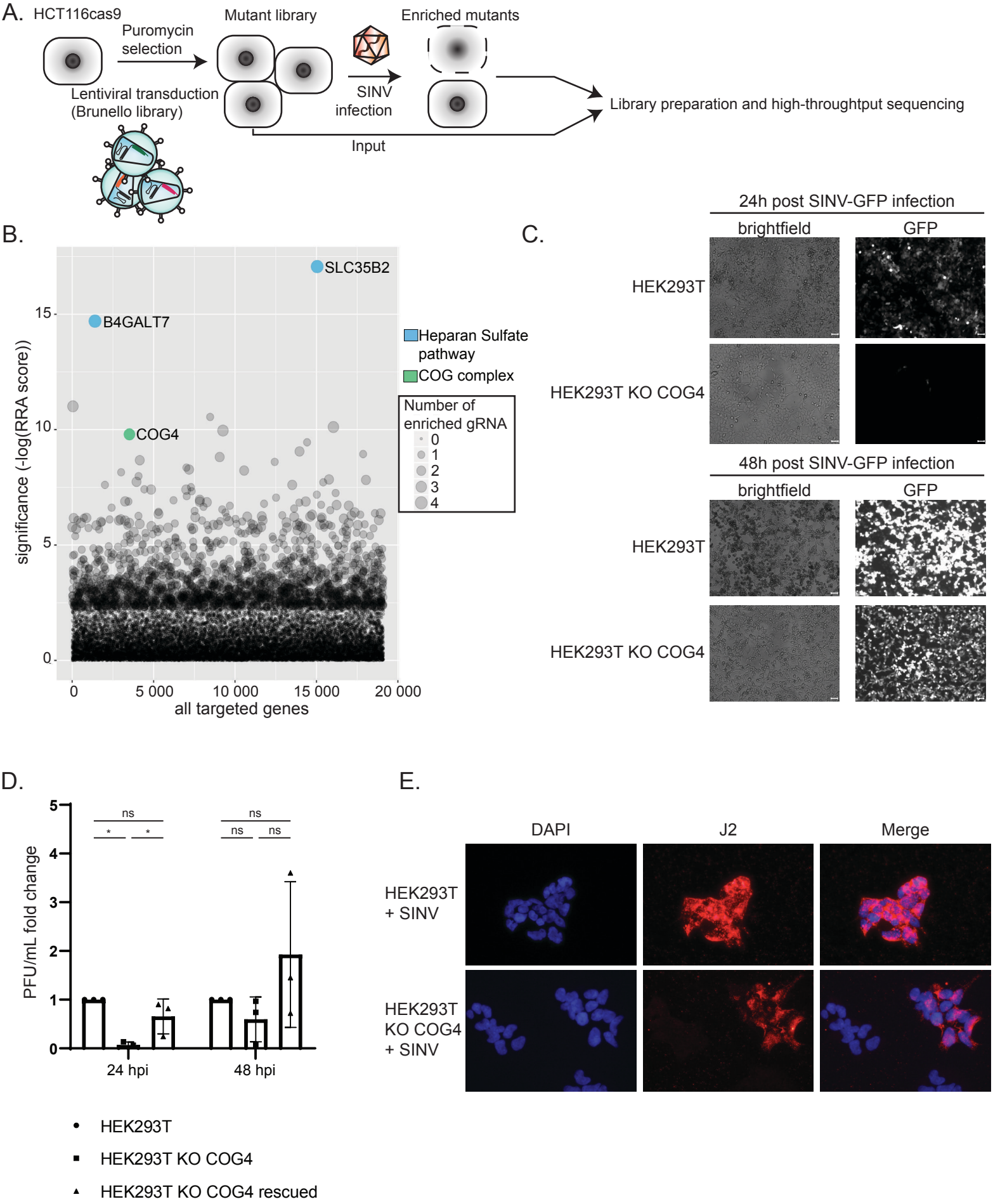

Petitjean et al., Figure 3

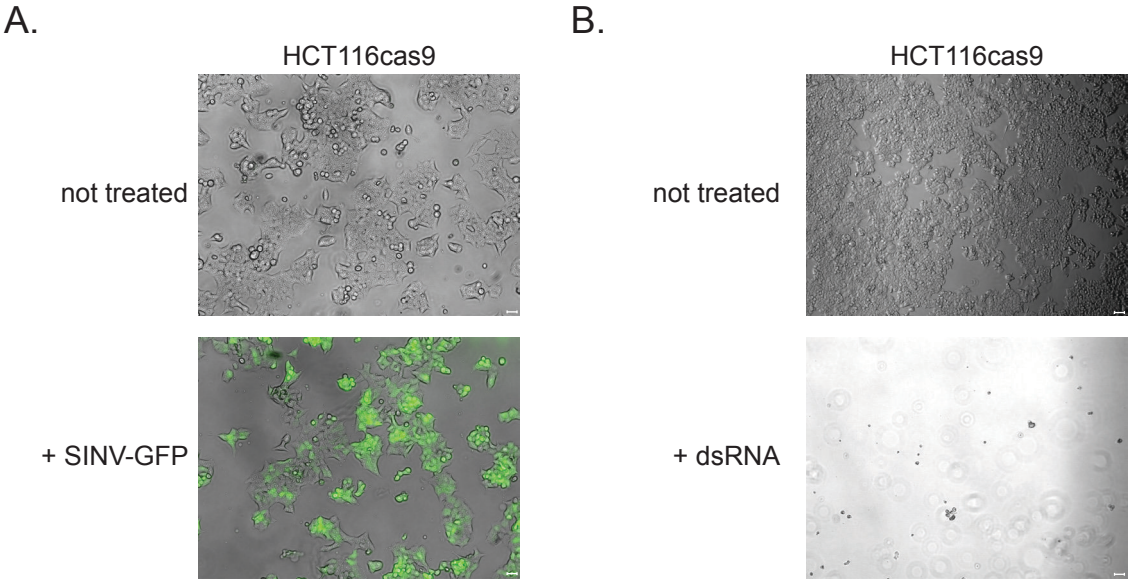

Petitjean et al., Figure S1

A.

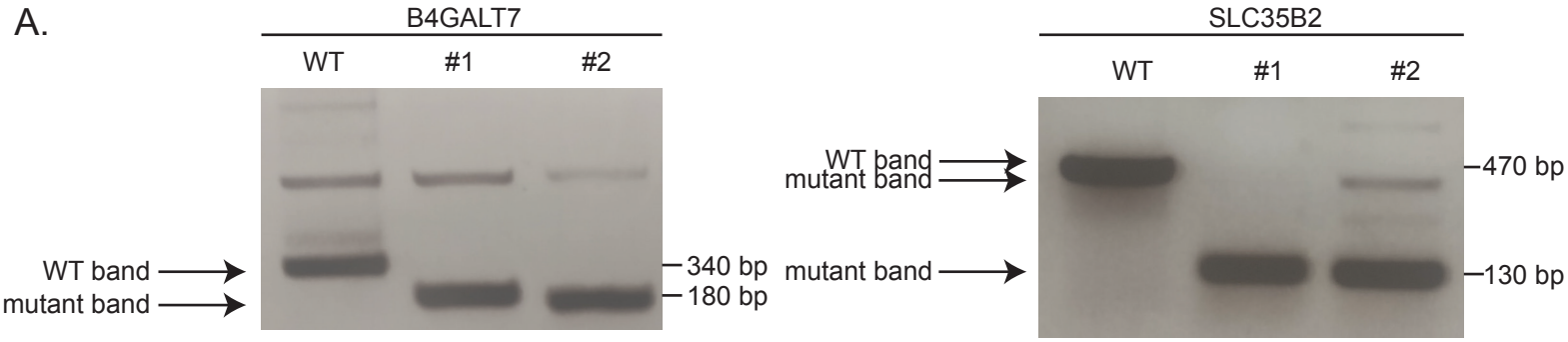

B.

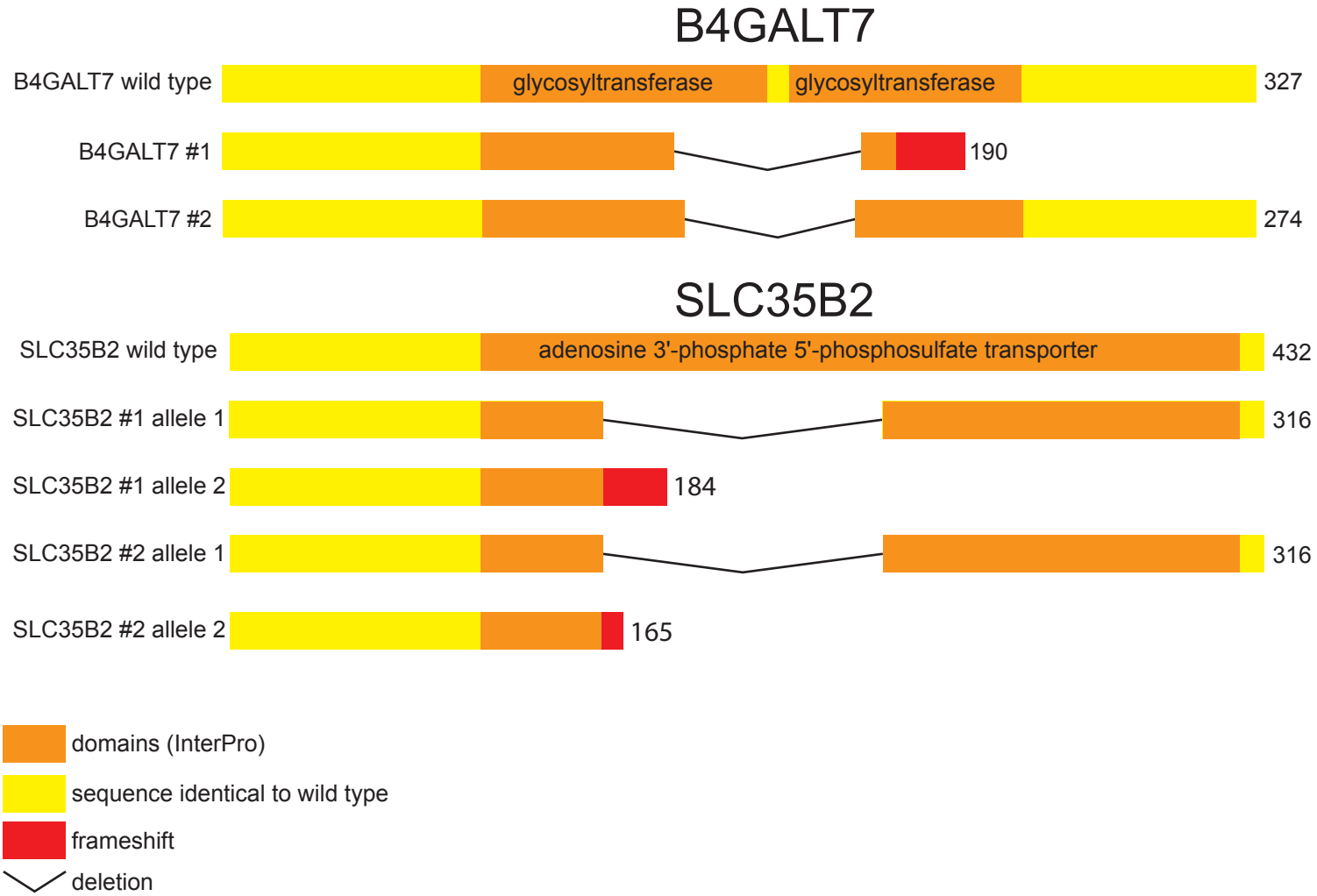

Petitjean et al., Figure S2

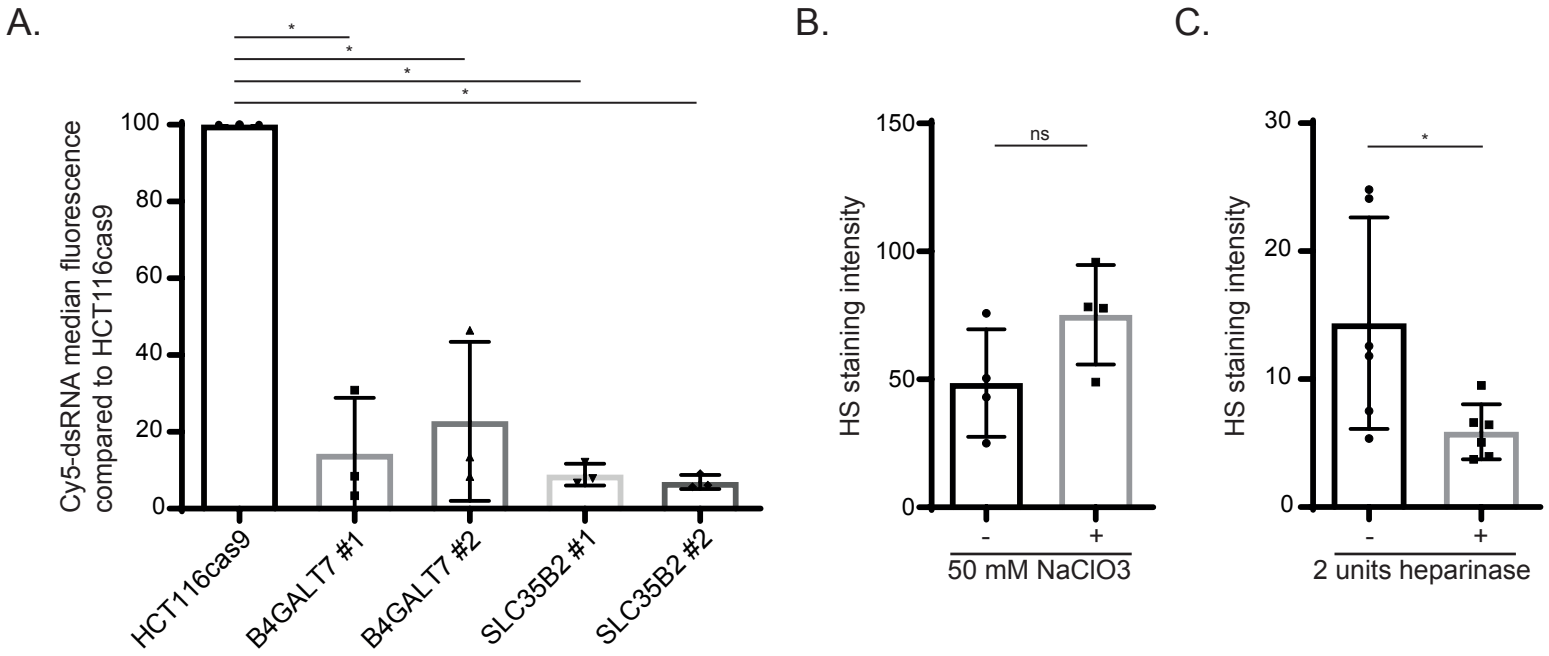

Petitjean et al., Figure S3

A.

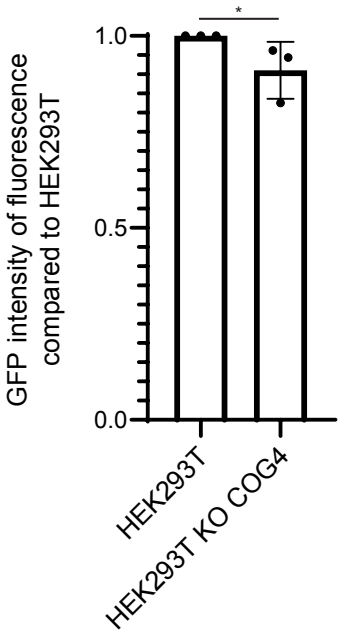

B.

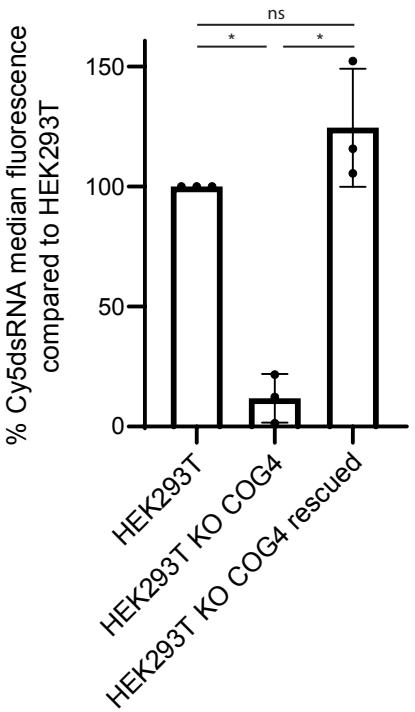

C.

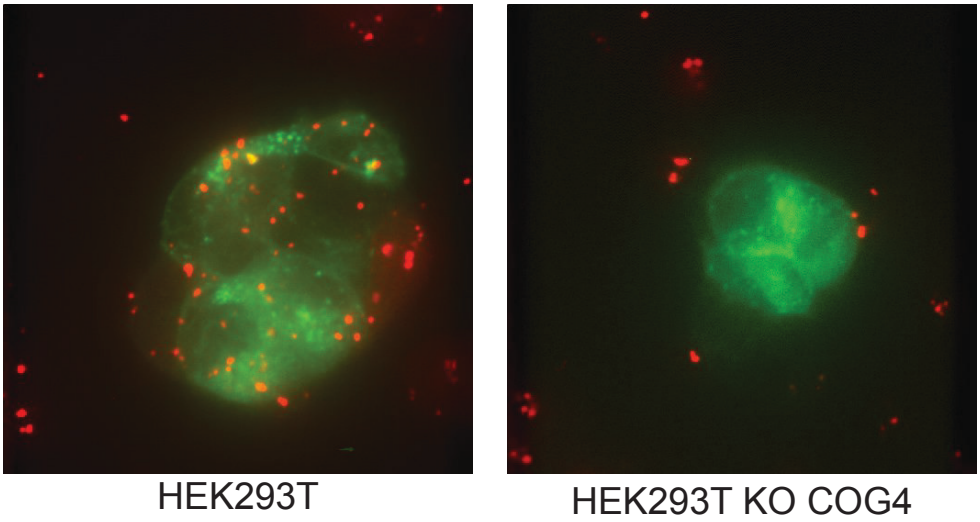

6 hours post poly(I:C) rhodamine transfection

D.

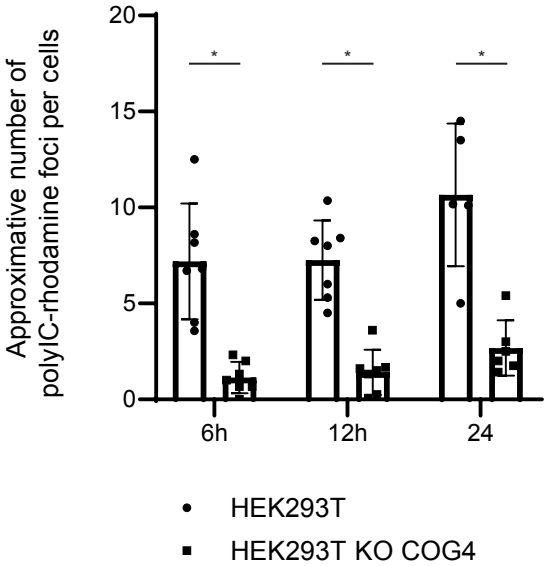

Petitjean et al., Figure S4

Type	Primer name	Sequence (5' -> 3')
gRNA sequences	B4GALT7 gRNA sequence 1	CACTACAAGACCTATGTCGG
	B4GALT7 gRNA sequence 2	CGGGCAGCGCTCATCAACGT
	SLC35B2 gRNA sequence 1	GCACTCGGTTCATTAGCACC
	SLC35B2 gRNA sequence 2	TATAACCTGCCAGTAAGATG
PCR primer to screen KO	B4GALT7 KO forward	AGTCAGTGCTGGGCCAGAGG
	B4GALT7 KO reverse	CAGCCGGTAGTGCTGCTTGG
	SLC35B2 KO forward	GGGGCCACAGCCACATCACC
	SLC35B2 KO reverse	AGGCAAACAGGGCATCCTGC
CRISPR screen primers	Crispr_lib_Seq_F01	AATGATACGGCGACCACCGAGATCTACACTCTTTCCCTACACGACGCTCTTCCGATCTTTGTGGAAAGGACGAAACACCG
	Crispr_lib_Seq_F02	AATGATACGGCGACCACCGAGATCTACACTCTTTCCCTACACGACGCTCTTCCGATCTCTTGTGGAAAGGACGAAACACCG
	Crispr_lib_Seq_F03	AATGATACGGCGACCACCGAGATCTACACTCTTTCCCTACACGACGCTCTTCCGATCTGCTTGTGGAAAGGACGAAACACCG
	Crispr_lib_Seq_F04	AATGATACGGCGACCACCGAGATCTACACTCTTTCCCTACACGACGCTCTTCCGATCTAGCTTGTGGAAAGGACGAAACACCG
	Crispr_lib_Seq_F05	AATGATACGGCGACCACCGAGATCTACACTCTTTCCCTACACGACGCTCTTCCGATCTCAACTTGTGGAAAGGACGAAACACCG
	Crispr_lib_Seq_F06	AATGATACGGCGACCACCGAGATCTACACTCTTTCCCTACACGACGCTCTTCCGATCTTGCACCTTGTGGAAAGGACGAAACACCG
	Crispr_lib_Seq_F07	AATGATACGGCGACCACCGAGATCTACACTCTTTCCCTACACGACGCTCTTCCGATCTACGCAACTTGTGGAAAGGACGAAACACCG
	Crispr_lib_Seq_F08	AATGATACGGCGACCACCGAGATCTACACTCTTTCCCTACACGACGCTCTTCCGATCTGAAGACCCTTGTGGAAAGGACGAAACACCG
	Crispr_lib_R01	CAAGCAGAAGACGGCATACGAGATAAGTAGAGGTGACTGGAGTTCAGACGTGTGCTCTTCCGATCTTCTACTATTCTTTCCCCTGCACTGT
	Crispr_lib_R02	CAAGCAGAAGACGGCATACGAGATACACGATCGTGACTGGAGTTCAGACGTGTGCTCTTCCGATCTTCTACTATTCTTTCCCCTGCACTGT
	Crispr_lib_R03	CAAGCAGAAGACGGCATACGAGATCGCGCGGTGTGACTGGAGTTCAGACGTGTGCTCTTCCGATCTTCTACTATTCTTTCCCCTGCACTGT
	Crispr_lib_R04	CAAGCAGAAGACGGCATACGAGATCATGATCGGTGACTGGAGTTCAGACGTGTGCTCTTCCGATCTTCTACTATTCTTTCCCCTGCACTGT
	Crispr_lib_R05	CAAGCAGAAGACGGCATACGAGATCGTTACCAGTGACTGGAGTTCAGACGTGTGCTCTTCCGATCTTCTACTATTCTTTCCCCTGCACTGT
	Crispr_lib_R06	CAAGCAGAAGACGGCATACGAGATTCCTTGGTGTGACTGGAGTTCAGACGTGTGCTCTTCCGATCTTCTACTATTCTTTCCCCTGCACTGT
	Crispr_lib_R07	CAAGCAGAAGACGGCATACGAGATAACGCATTGTGACTGGAGTTCAGACGTGTGCTCTTCCGATCTTCTACTATTCTTTCCCCTGCACTGT
	Crispr_lib_R08	CAAGCAGAAGACGGCATACGAGATACAGGTATGTGACTGGAGTTCAGACGTGTGCTCTTCCGATCTTCTACTATTCTTTCCCCTGCACTGT
	Crispr_lib_R09	CAAGCAGAAGACGGCATACGAGATAGGTAAGGGTGACTGGAGTTCAGACGTGTGCTCTTCCGATCTTCTACTATTCTTTCCCCTGCACTGT
dsRNA production	dsRNA Positive strand	GAAATTAATACGACTCACTATAGGCCATGCCCGAAGGCTACGTC
		TGTCGGCCATGATATAGACG
	dsRNA Negative strand	CCATGCCCGAAGGCTACGTC
		GAAATTAATACGACTCACTATAGGTGTCGGCCATGATATAGACG
qPCR primers	qPCR GAPDH	5'CCAGTGAGCTTCCCGTTCAG'3
		5'CTTTGGTATCGTGGAAGGACT'3
	qPCR dsRNA	GAACCGCATCGAGCTGAA
		CTACAACAGCCACAACGTCTA